JOC Article
pubs.acs.org/joc

The Effect of Structure on Nitroxide EPR Spectral Linewidth

Scott R. Burks,[†,‡] Mallory A. Makowsky,[§] Zachary A. Yaffe,[§] Chad Hoggle,[§] Pei Tsai,[†,§] Sukumaran Muralidharan,[†] Michael K. Bowman,[∥] Joseph P.Y. Kao,[†,‡] and Gerald M. Rosen*[,†,§]

[†]*Center for Biomedical Engineering and Technology, and Center for EPR Imaging In Vivo Physiology, University of Maryland, Baltimore, Maryland 21201,* [‡]*Department of Physiology, University of Maryland School of Medicine, Baltimore, Maryland 21201,* [§]*Department of Pharmaceutical Sciences, University of Maryland School of Pharmacy, Baltimore, Maryland 21201, and* [∥]*Department of Chemistry, The University of Alabama, Tuscaloosa, Alabama 35487*

grosen@umaryland.edu

Received March 25, 2010

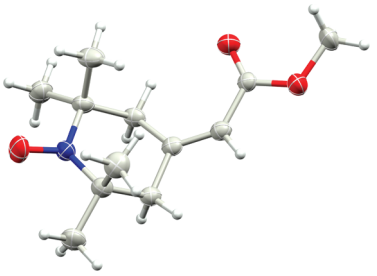

Nitroxides with narrow linewidths are essential for low-frequency EPR spectroscopy and in vivo EPR imaging. In developing a framework for designing narrow-line nitroxides, we sought to understand the unexpectedly narrow line width of 4-oxo-2,2,6,6-tetramethyl-1-piperidinyloxyl (**5**). Computational modeling revealed that the carbonyl double bond in the 4-position allows conformational diversity that results in the observed narrowing of the EPR spectral line. In view of this finding, we synthesized two new nitroxides bearing an exocyclic double bond: 4-methoxycarbonylmethylidene-2,2,6,6-tetramethyl-1-piperidinyloxyl (**7**) and 4-acetoxymethoxycarbonylmethylidene-2,2,6,6-tetramethyl-1-piperidinyloxyl (**9**). These nitroxides, like nitroxide **5**, exhibited narrow linewidths—consistent with the results of modeling. Nitroxide **8** (4-carboxymethylidene-2,2,6,6-tetramethyl-1-piperidinyloxyl), as a prototype, allows for a variety of structural diversity, such as nitroxide **9**,that can, for instance, target tissue compartments for in vivo EPR imaging.

Introduction

With the design and construction of low-frequency EPR spectrometers[1] that can detect paramagnetic species in living animals in real time, one of the challenges has been the synthesis of stable free radicals with narrow spectral linewidths for specific physiologic measurements, such as quantifying O_2 levels in discrete tissues[2] or targeting tumors[3] in vivo. For example, low-frequency EPR oximetry images can be derived from measuring the O_2-dependent broadening of the EPR spectral line of a trityl radical in each image voxel. Such measurement allows real-time quantification of O_2 in tumors in vivo.[2c] However, the trityl radicals used in these measurements are highly charged and do not enter the intracellular volume of tumor cells and, thus, are confined to the vasculature of the tumor. Therefore, the trityl oximetric images report O_2 in the extracellular, not intracellular, compartment.[2c] For more refined oximetry studies that enable imaging of intracellular

(1) (a) Halpern, H. J.; Spencer, D. P.; van Polen, J.; Bowman, M. K.; Massoth, R. J.; Nelson, A. C.; Dowey, E. M.; Teicher, B. A. *Rev. Sci. Instrum.* **1989**, *60*, 1040–1050. (b) Halpern, H. J.; Bowman, M. K. In *EPR Imaging and In Vivo EPR*; Eaton, G. R., Eaton, S. S., Ohno, K., Eds.; CRC Press: Boca Raton, 1991; pp 45−63.

(2) (a) Halpern, H. J.; Yu, C.; Peric, M.; Barth, E.; Grdina, D. J.; Teicher, B. A. *Proc. Natl. Acad. Sci. U.S.A.* **1994**, *91*, 13047–13051. (b) Halpern, H. J.; Yu, C.; Peric, M.; Barth, E. D.; Karczmar, C. S.; River, J. N.; Grdina, D. J.; Teicher, B. A. *Radiat, Res.* **1996**, *145*, 610–618. (c) Elas, M.; Williams, B. B.; Parasca, A.; Mailer, C.; Pelizzari, C. A.; Lewis, M. A.; River, J. N.; Karczmar, C. S.; Barth, E. D.; Halpern, H. J. *Magn. Reson, Med.* **2003**, *49*, 682–691.

(3) (a) For a review on this topic, see: Swartz, H. M.; Sentjurc, M.; Kocherginsky, N. In *Nitroxide Spin Labels. Reactions in Biology and Chemistry*; CRC Press: Boca Raton, 1995; pp 175−198. (b) Griffeth, L. K.; Rosen, G. M.; Rauckman, E. J.; Drayer, B. P. *Invest. Radiol.* **1984**, *19*, 553–562.

DOI: 10.1021/jo1005747 Published on Web 06/11/2010

O_2, it is important to design spin probes that can diffuse from the tumor vasculature and be retained in the constituent tumor cells.

Nitroxides have proven to be an important class of free radical probes for physiological studies.[3] They have been employed to study membrane fluidity and redox status of isolated cells.[3a] The relaxivity of nitroxides has been useful in measuring the in vivo redox state of tissues through both Overhauser enhanced MRI[4] and high-field MRI.[5] Nitroxides have found limited application in EPR imaging, owing in part to their large intrinsic line width, which limits the spatial resolution of EPR images. In the 1970s, Ramasseul and Rassat[6a] synthesized pyrroloxyls that exhibited narrow linewidths in the absence of oxygen; the linewidths were found to be proportional to the square of the isotropic hyperfine coupling of the nitrogen, A_N. These pyrroloxyls prompted us to investigate the synthesis of similar nitroxides as possible in vivo EPR imaging agents. To our surprise, we found that the reported oxidation of 2,5-di(*tert*-butyl)-3-ethoxycarbonyl-1-hydroxypyrrole (**1**) by nickel peroxide[6] actually yielded two products: 2,5-di(*tert*-butyl)-3-ethoxycarbonyl-4-hydroxy-1-pyrroloxyl (**2**) and 2,2′,5,5′-tetra(*tert*-butyl)-4,4′-bis(ethoxycarbonyl)-3,3′-bipyrrolyl-1,1′-dioxyl (**3**).[7] However, neither of these nitroxides is suitable as an in vivo EPR imaging agent. Pyrroloxyl **2** is unstable and is rapidly oxidized to the corresponding *N*-oxide **4**.[7] Despite the stability of biradical **3**, it is not sufficiently water-soluble to permit in vivo EPR imaging studies. We therefore sought alternative nitroxides that have narrow linewidths.

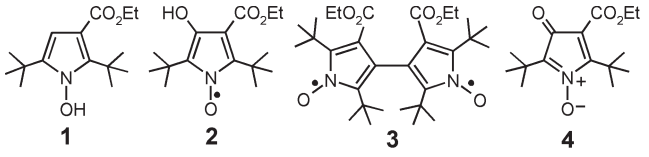

Saito and colleagues previously reported[8] that the linewidth of 4-oxo-2,2,6,6-tetramethyl-1-piperidinyloxyl (**5**) in phosphate buffer is remarkably small at 0.47 G, in stark contrast to 4-hydroxy-2,2,6,6-tetramethyl-1-piperidinyloxyl (**6**), whose line width is 1.58 G under identical conditions. The two nitroxides have A_N values of 15.9 and 16.9 G, respectively. Clearly the difference in linewidths does not follow the A_N-squared relation as reported for the pyrroloxyls. We wish to understand the difference in linewidths of nitroxides **5** and **6** and ultimately to design new nitroxides with narrow linewidths that can be readily conjugated to other moieties for targeting specific cell types or tissue compartments for in vivo EPR imaging. Here, we describe the synthesis of one such piperidinyloxyl, with an exocyclic double bond, that retains the narrow line width of nitroxide **5** and that bears a functional group that can be elaborated for diverse applications.

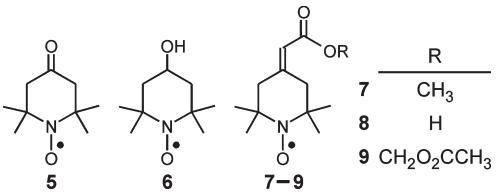

Results and Discussion

The lineshapes of nitroxides have been studied extensively because of their dependence on molecular motion in liquids. In the fast motional regime (applicable to an aqueous solution at room temperature), nitroxides **5** and **6** have three well-resolved lines in their EPR spectra. The width of each line has four main contributions: rotational modulation of anisotropic hyperfine and *g*-factor interactions, inhomogeneous broadening by unresolved hydrogen hyperfine couplings, exchange broadening from collisions with paramagnetic molecules, and spin-rotation coupling. The empirical correlation reported[7] between linewidth and A_N arises from the strong correlation between A_N and the anisotropic hyperfine tensor.

Dynamic averaging made possible by conformational flexibility significantly reduces the linewidths of nitroxides **5** and **7** from the 1.44 G predicted for the rigid conformation (Table 1). The exchange broadening and spin-rotational couplings are not major contributors to the linewidths reported for nitroxides **5** and **6** or under typical EPR imaging conditions. This leaves rotational modulation of anisotropic interactions and inhomogeneous broadening as the probable sources of the observed linewidths. The *g*-factors and hyperfine-tensors of nitroxides **5** and **6** are quite similar and do not account for the difference in observed linewidths. The remaining source of the difference in linewidths is the inhomogeneous broadening by unresolved hydrogen hyperfine couplings in the nitroxide. The hydrogen hyperfine splittings can be substantially reduced by complete deuteration of the nitroxide and is commonly employed for EPR imaging, yet even the deuterated linewidth remains a limiting factor. Any decrease in the hydrogen hyperfine contribution to the linewidth would also improve the performance of the deuterated analog.

Hydrogen hyperfine couplings from density functional theory (DFT) calculations for the lowest energy structures of nitroxides **5** and **6** are presented in the first three columns of Table 1; methyl groups in the molecules are assumed to be rapidly rotating. The calculated hydrogen contribution to the linewidths of nitroxides **5** and **6** is remarkably similar at about 1.44 G. The substituents in the 4-position have offsetting effects on the distribution of unpaired spin density so that the overall linewidth is essentially constant.

The minimum energy conformation of nitroxides **5** and **6** has two or four symmetry-related structures, in which hydrogen atoms and methyl groups that are axial with respect to the ring become equatorial and vice versa. The hyperfine couplings will be averaged for symmetry-related positions if the rate of conformational interchange is much greater than 10^7 s^{-1}. In nitroxide **5**, for example, the methyl group couplings of 0.286 and −0.431 G average to −0.073 G. Because the axial and equatorial A_H have opposite signs, conformational interchange results in substantial reductions in hyperfine

(4) Utsumi, H.; Yanada, K.; Ichikawa, K.; Sakat, K.; Kinoshita, Y.; Matsumoto, S.; Nagai, M. *Proc. Natl. Acad. Sci. U.S.A.* **2002**, *99*, 2216–2221.
(5) Matsumoto, K.; Hyodo, F.; Matsumoto, A.; Koretsky, A. P.; Sowers, A. L.; Mitchell, J. B.; Krishna, M. C. *Clin. Cancer Res.* **2006**, *12*, 2455–2462.
(6) (a) Ramasseul, R.; Rassat, A. *Bull. Soc. Chim. Fr.* **1970**, *72*, 4330–4340. (b) Radner, F.; Rassat, A.; Hersvall, C.-J. *Acta Chem. Scand.* **1996**, *50*, 146–149.
(7) Riplinger, C.; Kao, J. P. Y.; Rosen, G. M.; Kathirvelu, V.; Eaton, G. R.; Eaton, S. S.; Kutateladze, A.; Neese, F. *J. Am. Chem. Soc.* **2009**, *131*, 10092–10106.
(8) Saito, K.; Takeshita, K.; Ueda, J.-I; Ozawa, T. *J. Pharm. Sci.* **2003**, *92*, 275.

TABLE 1. Hydrogen Hyperfine Couplings[a] for Nitroxides 5−8

	rigid				symmetry-averaged			
	5	**6**	**7**	**8**	**5**	**6**	**7**	**8**
axial $-CH_3$	0.286	0.277	0.314	0.286	−0.073	−0.083	−0.045	−0.064
axial $-CH_3$	0.286	0.202	0.199	0.240	−0.073	−0.105	−0.045	−0.064
equatorial $-H_3$	−0.431	−0.413	−0.404	−0.415	−0.073	−0.083	−0.127	−0.102
equatorial $-CH_3$	−0.431	−0.442	−0.452	−0.443	−0.073	−0.105	−0.127	−0.102
axial $>CH_2$	−0.295	−0.288	−0.337	−0.324	0.041	0.006	0.120	0.079
axial $>CH_2$	−0.295	−0.272	−0.272	−0.271	0.041	0.192	−0.031	0.079
equatorial $>CH_2$	0.374	0.655	0.577	0.483	0.041	0.192	0.120	0.022
equatorial $>CH_2$	0.378	0.300	0.210	0.315	0.041	0.006	−0.031	0.022
linewidth	1.44	1.46	1.44	1.43	0.27	0.43	0.37	0.32

[a]Calculated with Gaussian-03 or Gaussian-09 at the ublyp3/TZVP//ub3lyp/6-31G* level. Values of A_H are in gauss. Linewidth contributions from the hydrogens are calculated from the hydrogen hyperfine second moment.

SCHEME 1

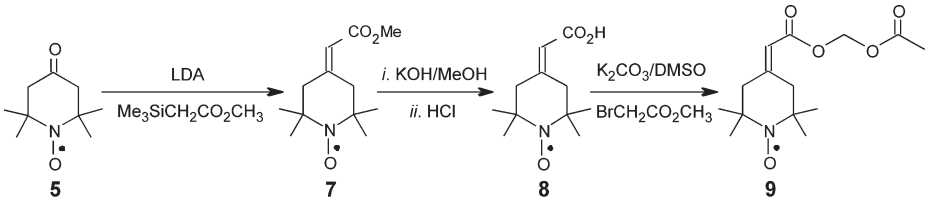

splittings, $|A_H|$, and in smaller linewidths (Table 1, symmetry-averaged columns).

Dynamic averaging made possible by conformational flexibility significantly reduces the linewidths of nitroxides **5** and **6** from the predicted linewidth for the rigid conformation. The dramatic reduction does not result from the molecule adopting some average symmetric planar structure because such a planar structure has appreciable methyl hydrogen hyperfine splittings. Rather, the fluctuations converting axial methyl groups with positive A_H into an equatorial configuration with negative A_H dynamically average the couplings to a very small value, resulting in a narrow line width. The 4-OH group in nitroxide **6** preferentially occupies an equatorial position and prevents the full conformational averaging found in nitroxide **5**; the consequence is a larger line width. These findings indicate that the 4-position in a six-membered nitroxide needs to have two identical substituents or a double bond to enable the conformational averaging needed for narrow linewidths.

In a nitroxide with adequate flexibility to enable the α-methyl groups to interchange rapidly between conformations that are nearly perpendicular and nearly parallel to the ring, there are significant contributions from intermediate conformations. The experimental linewidth will reflect averaging of all accessible conformations and not just the symmetry-related lowest-energy conformations. Therefore, the predicted linewidths can only be expected to estimate general trends.

We surmised that a double-bonded substituent at the 4-position of a piperidinyloxyl should allow the dynamic averaging of hydrogen hyperfine couplings needed for a narrow line width. We therefore incorporated at the 4-position an exocyclic double bond bearing a functional group that would allow further synthetic modifications. Such modifications could be designed to target the nitroxide to specific cellular compartments. Our approach is based on literature precedents from us and others.[9] Previously, we had synthesized the *tert*-butyl ester analogue of **7**, 4-*tert*-butoxycarbonylmethylidene-2,2,6,6-tetramethyl-1-piperidinyloxyl, by first preparing lithio *tert*-butyl trimethylsilylacetate, to which nitroxide **5** was added in a Wittig-type reaction. Reaction of nitroxide **5** with lithio methyl trimethylsilylacetate at −78 °C was similarly successful, affording nitroxide **7** in reasonable yield (Scheme 1). The molecular structure of **7** was determined by X-ray crystallographic analysis (Figure 1)

TABLE 2. EPR Splitting Constants and Linewidths for Nitroxides 5−9[a]

	5	**6**	**7**	**8**	**9**
linewidth[b]	0.76	1.60	0.92	0.98	0.93
A_N	15.78	16.66	16.34	16.42	16.34

[a]All values in units of gauss. [b]Peak-to-peak EPR spectral linewidths. See the Experimental Section for details.

A successful spin probe for EPR imaging is one that can be readily loaded into cells at high concentrations and be retained intracellularly for long periods of time. We demonstrated that an acetoxymethyl ester, but not the methyl ester, of a nitroxide is readily hydrolyzed to the corresponding carboxylate by intracellular esterases, enabling intracellular entrapment after diffusion through the cell membrane.[10] Sufficiently high levels of nitroxide are accumulated in the mouse brain through this mechanism to permit quantitation of O_2 levels through EPR imaging.[11] Guided by this earlier success, we prepared the acetoxymethyl ester, nitroxide **9**, by first hydrolyzing nitroxide **7** under mild conditions to yield the acid **8**. Alkylating nitroxide **8** with bromomethyl acetate afforded the corresponding acetoxymethyl ester **9** (Scheme 1).

Like nitroxide **7**, nitroxides **8** and **9** have experimental linewidths closer to that of **5** than to **6** (Table 2). DFT calculations

(9) (a) Rosen, G. M.; Rauckman, E. J. *Org. Prep. Proc. Int.* **1978**, *10*, 17–20. (b) Shimoji, K.; Taguchi, H.; Oshima, K.; Yamamoto, H.; Nozaki, H. *J. Am. Chem. Soc.* **1974**, *96*, 1620–1621.

(10) (a) Kao, J. P. Y.; Rosen, G. M. *Org. Biomol. Chem.* **2004**, *2*, 99–102. (b) Rosen, G. M.; Burks, S. R.; Kohr, M. J.; Kao, J. P. Y. *Org. Biomol. Chem.* **2005**, *3*, 645–648. (c) Shen, J.; Liu, S.; Miyake, M.; Liu, W.; Pritchard, A.; Kao, J. P. Y.; Rosen, G. M.; Tong, Y.; Liu, K. J. *Magn. Reson. Med.* **2006**, *55*, 1433–1440.

(11) Shen, J.; Sood, R.; Weaver, J.; Timmins, G. S.; Schnell, A.; Miyake, M.; Kao, J. P. Y.; Rosen, G. M.; Liu, K. J. *J. Cereb. Blood Flow Metab.* **2009**, *29*, 1695–1703.

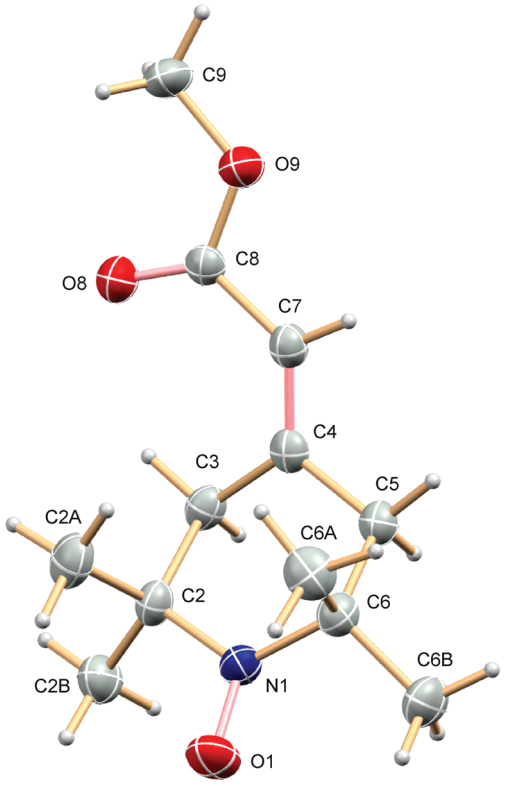

FIGURE 1. Molecular structure of nitroxide **7** determined by X-ray crystallography.

show hydrogen hyperfine couplings consistent with those of nitroxides **5** and **6**, and more importantly, no significant couplings to the exocyclic vinylic hydrogen. Therefore, in applications where the acetoxymethyl ester **9** and similar nitroxides are used for a variety of imaging studies, the new compounds can be expected to have relatively small hydrogen hyperfine contributions to linewidth and are thus valuable probes for in vivo EPR imaging studies.

Experimental Section

General Methods. Chemicals were of reagent grade unless indicated otherwise. For column chromatography, silica gel was used (230−400 mesh). 4-Hydroxy-2,2,6,6-tetramethyl-1-piperidinyloxyl (**6**) was purchased.

4-Methoxycarbonylmethylidene-2,2,6,6-tetramethyl-1-piperidinyloxyl (7). *n*-BuLi (2.5 M in hexane, 2.9 mL, 7.1 mmol) was added to a three-necked flask containing THF (50 mL, freshly distilled over $LiAlH_4$) at −5 °C under N_2 atmosphere. Then, diisopropylamine (1.0 mL, 7.1 mmol) in THF (5 mL) was added; care was taken to maintain the temperature at −5 °C. Thereafter, the flask was immersed in a dry ice−acetone bath at −78 °C and methyl 2-(trimethylsilyl)acetate (97%, 1.2 mL, 7.1 mmol) dissolved in THF (20 mL) was added slowly, with the reaction mixture being maintained at −78 °C. After the addition was complete, stirring was continued at −78 °C for 20 min before 2,2,6,6-tetramethyl-4-oxo-1-piperidinyloxyl (**5**) (1.2 g, 7.1 mmol, prepared as previously reported;[12] purified on silica gel, 2:1 hexane/Et_2O) in THF (20 mL) was added to the reaction. After 20 min, the mixture was warmed to room temperature. Cold 5% HCl was added to attain a pH of 3−4, and the mixture was extracted with 1:1 pentane/Et_2O (3 times). The combined organic solutions were washed with saturated aqueous Na_2CO_3, dried over anhydrous Na_2SO_4, and evaporated to dryness to yield thick red oil. This oil was eluted from silica gel with 4:1 hexane/Et_2O to give 4-methoxycarbonylmethylidene-2,2,6,6-tetramethyl-1-piperidinyloxyl (**7**) as a red oil, which eventually solidified (1.2 g, 75%; mp = 57−58 °C after recrystallization from hexane): IR ($CHCl_3$) 1713 (C=O), 1661 (C=C) cm^{-1}. Crystals of **7** were used for X-ray crystallographic structure determination (see below).

4-Acetoxymethoxycarbonylmethylidene-2,2,6,6-tetramethyl-1-piperidinyloxyl (9). To a solution of 4-methoxycarbonylmethylidene-2,2,6,6-tetramethyl-1-piperidinyloxyl (**7**) (1 g, 4.4 mmol) in 25 mL of methanol were added KOH (0.25 g, 4.4 mmol) and H_2O (2 mL). The reaction was warmed (< 40 °C) for 6 h; progress of hydrolysis was monitored by TLC (silica gel; 1:1 hexane/Et_2O). Upon cooling to room temperature, the reaction mixture was evaporated to dryness in vacuo. H_2O (50 mL) was added, and the mixture was extracted with CH_2Cl_2 (3 × 25 mL). The aqueous solution was then cooled in an ice bath, and the pH was adjusted to between 3 and 4 with 10% HCl. The solution was then extracted with ether, dried over anhydrous $MgSO_4$, and evaporated under vacuum to yield 4-carboxymethylidene-2,2,6,6-tetramethyl-1-piperidinyloxyl (**8**) as a red oil, which was used for EPR spectroscopy. Compound **8** was used directly for preparing the acetoxymethylester **9**: K_2CO_3 (1.4 g, 10.2 mmol) was added to a solution of the acid **8** (1.08 g, 5.1 mmol) in DMSO (5 mL), and the mixure was stirred at room temperature for 10 min. Bromomethyl acetate (0.78 g, 0.5 mL, 5.1 mmol) was then added, and the mixture was stirred for 3 h. Thereafter, CH_2Cl_2 (50 mL) was added, and the solution was washed with H_2O (3 × 100 mL). The organic phase was dried over anhydrous Na_2SO_4 and evaporated to dryness to yield a thick red oil. Chromatography on silica gel (25:6 hexane/EtOAc) gave 4-acetoxymethoxycarbonylmethylidene-2,2,6,6-tetramethyl-1-piperidinyloxyl (**9**), as a thick red oil (0.75 g, 50%): IR ($CHCl_3$) 1757, 1733 (C=O), 1653 (C=C) cm^{-1}. Anal. Calcd for $C_{14}H_{22}NO_5$: C, 59.14; H, 7.80; N, 4.93. Found: C, 59.31; H, 7.69; N, 4.96.

EPR Spectroscopy. Spectra were acquired in a quartz flat-cell cuvette using an X-band EPR spectrometer. Nitroxides (10 μM) were dissolved into H_2O containing DMSO (10% v/v). Spectra were obtained using the following spectrometer settings: magnetic field, 333.5 mT; microwave frequency, 9.5 GHz; microwave power, 20 mW; modulation amplitude, 0.0125 mT: modulation frequency, 100 kHz; time constant, 0.5 s; scan rate, 2.67 mT/min. A range of 0.8 mT was digitized with 1000 points uniformly spaced in the magnetic field range. Data acquisition and digitization were performed using EWWIN software and data acquisition module. Reported spectral linewidths represent the peak-to-peak line width of the central peak in the nitroxide triplet spectrum.

X-ray Crystallography. X-ray crystallography was performed at the X-ray Crystallographic Center in the Department of Chemistry and Biochemistry at the University of Maryland, College Park. X-ray intensity data were measured at 250 ± 2 K on a 3-circle diffractometer equipped with a CCD area detector and a Mo Kα fine-focus sealed tube source (λ = 0.71073 Å) in conjunction with a graphite monochromator.

A red crystal of nitroxide **7**, measuring approximately 0.40 × 0.50 × 0.53 mm^3, was used for X-ray crystallographic analysis. Over 25.9 h, 1830 data frames were collected with a scan width of −0.30° in ω and an exposure time of 45 s/frame. The frames were integrated with the Apex2 software package using a narrow-frame integration algorithm. Data were corrected for absorption effects with the semiempirical equivalents method using SADABS software.[13] Integration of the data using a monoclinic

(12) Rozantsev, E. G. *Free Nitroxyl Radicals*; Plenum Press: New York, 1970; p 208.

(13) Sheldririck, G. M. *SADABS*; University of Göttingen: Göttingen, 1996.

unit cell yielded a total of 9232 reflections (maximum θ of 25.00°), of which 2268 were independent (100% completeness, R_{int} = 2.20%, R_{sig} = 2.16%) and 1909 were greater than $2\sigma(I)$. The final cell dimensions of a = 7.7657(7) Å, b = 15.5387(14) Å, c = 11.2639(10) Å, $\alpha = \gamma = 90°$, β = 109.5925(10)°, and V = 1280.5(2) Å^3 are based on the refinement of the XYZ-centroids of 5154 reflections with $2.3 < \theta < 25.5°$. Analysis of the data showed 0% decay during data collection. The minimum and maximum transmission coefficients were 0.914 and 0.967.

The structure was solved and refined using SHELXS-97 and SHELXL-97 software[14a,b] in the space group $P2_1/c$ with $Z = 4$ for the formula unit $C_{12}H_{20}NO_3$. The final anisotropic full-matrix least-squares refinement on F^2 with 161 variables converged at R_1 = 4.88% for the observed data and wR_2 = 9.70% for all data. The goodness-of-fit was 1.000. The largest peak on the final difference map was 0.439 e$^-$/Å^3 and the largest hole was −0.157 e$^-$/Å^3. On the basis of the final model, the calculated density was 1.174 g·cm^{-3} and F(000), 492 e$^-$. Crystallographic details for nitroxide **9**, including atomic coordinates, anisotropic displacements, etc. are included in the Supporting Information.

Quantum Chemical Calculations. To examine the hydrogen hyperfine couplings in the nitroxides, a series of density functional theory (DFT) calculations were performed using Gaussian-03[15] and Gaussian-09.[16] The structures were optimized at the ub3lyp/6-31G** level and hyperfine couplings calculated with ub3lyp/TZVP. The methyl groups were assumed to be rapidly rotating so the Fermi contact couplings for the three hydrogens in each methyl group were averaged to give a single isotropic hyperfine coupling, A_H, for that methyl group.

Acknowledgment. This research was supported in part by National Institutes of Health Grant Nos. DA023473 and EB2034 (G.M.R.), GM061904 (M.K.B.), and GM056481 (J. P.Y.K.) and was made possible in part by a grant of high performance computing resources and technical support from the Alabama Supercomputer Authority.

Supporting Information Available: Tabulation of crystallographic information (atomic coordinates and displacements, bond lengths and angles); CIF; details of quantum mechanical calculations. This material is available free of charge via the Internet at http://pubs.acs.org.

(14) (a) Sheldrick, G. M. SHELXS97; University of Göttingen: Göttingen, 1997. (b) Sheldrick, G. M. SHELXL97; University of Göttingen: Göttingen, 1997.

(15) Gaussian 03, Revision C.02: Frisch, M. J.; Trucks, G. W.; Schlegel, H. B.; Scuseria, G. E.; Robb, M. A.; Cheeseman, J. R.; Montgomery, J. A., Jr.; Vreven, T.; Kudin, K. N.; Burant, J. C.; Millam, J. M.; Iyengar, S. S.; Tomasi, J.; Barone, V.; Mennucci, B.; Cossi, M.; Scalmani, G.; Rega, N.; Petersson, G. A.; Nakatsuji, H.; Hada, M.; Ehara, M.; Toyota, K.; Fukuda, R.; Hasegawa, J.; Ishida, M.; Nakajima, T.; Honda, Y.; Kitao, O.; Nakai, H.; Klene, M.; Li, X.; Knox, J. E.; Hratchian, H. P.; Cross, J. B.; Bakken, V.; Adamo, C.; Jaramillo, J.; Gomperts, R.; Stratmann, R. E.; Yazyev, O.; Austin, A. J.; Cammi, R.; Pomelli, C.; Ochterski, J. W.; Ayala, P. Y.; Morokuma, K.; Voth, G. A.; Salvador, P.; Dannenberg, J. J.; Zakrzewski, V. G.; Dapprich, S.; Daniels, A. D.; Strain, M. C.; Farkas, O.; Malick, D. K.; Rabuck, A. D.; Raghavachari, K.; Foresman, J. B.; Ortiz, J. V.; Cui, Q.; Baboul, A. G.; Clifford, S.; Cioslowski, J.; Stefanov, B. B.; Liu, G.; Liashenko, A.; Piskorz, P.; Komaromi, I.; Martin, R. L.; Fox, D. J.; Keith, T.; Al-Laham,M. A.; Peng, C. Y.; Nanayakkara, A.; Challacombe, M.; Gill, P. M. W.; Johnson, B.; Chen, W.; Wong, M. W.; Gonzalez, C.; Pople, J. A. Gaussian, Inc., Wallingford CT, 2004.

(16) Gaussian 09, Revision A.1: Frisch, M. J.; Trucks, G. W.; Schlegel, H. B.; Scuseria, G. E.; Robb, M. A.; Cheeseman, J. R.; Scalmani, G.; Barone, V.; Mennucci, B.; Petersson, G. A.; Nakatsuji, H.; Caricato, M.; Li, X.; Hratchian, H. P.; Izmaylov, A. F.; Bloino, J.; Zheng, G.; Sonnenberg, J. L.; Hada, M.; Ehara, M.; Toyota, K.; Fukuda, R.; Hasegawa, J.; Ishida, M.; Nakajima, T.; Honda, Y.; Kitao, O.; Nakai, H.; Vreven, T.; Montgomery, J. A., Jr.; Peralta, J.E.; Ogliaro, F.; Bearpark, M.; Heyd, J. J.; Brothers, E.; Kudin, K. N.; Staroverov, V. N.; Kobayashi, R.; Normand, J.; Raghavachari, K.; Rendell, A.; Burant, J. C.; Iyengar, S. S.; Tomasi, J.; Cossi, M.; Rega, N.; Millam, J. M.; Klene, M.; Knox, J. E.; Cross, J. B.; Bakken, V.; Adamo, C.; Jaramillo, J.; Gomperts, R.; Stratmann, R. E.; Yazyev, O.; Austin, A. J.; Cammi, R.; Pomelli, C.; Ochterski, J. W.; Martin, R. L.; Morokuma, K.; Zakrzewski, V. G.; Voth, G.A.; Salvador, P.; Dannenberg, J.J.; Dapprich, S.; Daniels, A. D.; Farkas, O.; Foresman, J. B.; Ortiz, J. V.; Cioslowski, J.; Fox, D. J. Gaussian, Inc., Wallingford, CT, 2009.